

A potpourri of results on molecular communication with active transport

Phanindra Dewan, Sumantra Sarkar

Abstract—Molecular communication (MC) is a model of information transmission where the signal is transmitted by information-carrying molecules through their physical transport from a transmitter to a receiver through a communication channel. Prior efforts have identified suitable “information molecules” whose efficacy for signal transmission has been studied extensively in diffusive channels (DC). Although easy to implement, DCs are inefficient for distances longer than tens of nanometers. In contrast, molecular motor-driven nonequilibrium or active transport can drastically increase the range of communication and may permit efficient communication up to tens of micrometers. In this paper, we investigate how active transport influences the efficacy of molecular communication, quantified by the mutual information between transmitted and received signals. We consider two specific scenarios: (a) active transport through relays and (b) active transport through a mixture of active and diffusing particles. In each case, we discuss the efficacy of the communication channel and discuss their potential pitfalls.

I. INTRODUCTION

COMMUNICATION systems are designed to transfer information across space and time. Therefore, any communication system must have a transmitter and a receiver of information and a channel to transmit the information to the receiver from the transmitter [1]. For example, during a telephonic conversation, the transmitter in a cellular phone transmits encoded information as an electromagnetic signal through the atmosphere (the channel), which is then received by the receiver on another phone and decoded. The quality of the received signal depends on the quality of the transmission and the reception circuitry and the atmospheric loss of the electromagnetic signal.

Modern technologies allow seamless electromagnetic communication in diverse conditions, yet in various situations of importance, electromagnetic wireless communication is unreliable or technologically difficult. For example, wireless communication is severely hindered in salty environments (such as through the ocean) or through cavernous regions (such as networks of tunnels, pipelines, or rooms). A common example is the presence of black spots in wifi networks, a source of everyday frustrations. Wireless communication is also challenging in extremely small spatial scales, such as in cellular environments, where communication is necessary

between nanoscale robots to identify and process some cells of interest. Building efficient nanoscale transmitters and receivers for electromagnetic communication is difficult. In any case, the salty cellular environments make the transmission lossy and inefficient. Therefore, in such situations, alternative modes of communication are needed.

Molecular communication (MC) is an alternative communication model where information is encoded in molecules and is carried by molecular transport through a channel. MCs require transmitters, receivers, channels, and information carriers like any communication system. Although some macroscopic realizations of MCs have been demonstrated [2], most experimental efforts have focused on creating “information molecules” and the channels through which they are transmitted [1, 3, 4]. For example, in kinesin-microtubule [5–10], or myosin-actin-based assays [11–13], vesicles attached to molecular motors can be thought of as the information molecule, and the filaments can be considered a network of 1D channels. Theoretical and modeling efforts have focused on various aspects of communication engineering, including modeling the receiver, the transmitter, and the channels [14–17]. Because of the presence of memory in MC channels, conventional theoretical treatments have been difficult [1]. However, several important discoveries have been made in understanding the consequences of transport in the so-called diffusion channels [7, 18–21, 21–34] and active, nonequilibrium channels [34, 35]. For example, in [21], the authors have looked at the practical feasibility of MC channels.

Another class of efforts has been targeted at understanding how channel capacity changes due to the mode of transport of the molecules [3, 4, 21, 33]. At the cellular level, the primary modes of transport are either diffusion or molecular motor-driven active transport [36]. Diffusion is an equilibrium transport process where molecules are transported through their incessant collision with the surrounding molecules, resulting in unbiased random walks. Active transport, in contrast, is a nonequilibrium transport process, where transport is facilitated by molecular motor proteins, which consume ATP to transport a molecule in a biased fashion [37]. A simple model for understanding active transport is a biased random walk. In a previous work [34], we investigated whether active transport is always a better option than diffusive transport in MC channels. We showed that diffusive transport is a better alternative for short communication channels, which may have led to the evolution of the cellular signaling cascades found in modern cells. For example, in bacteria, where the communication distances are shorter, two-step DCs are predominant, whereas, in eukaryotes, where the communication has to be carried over much larger distances, signals are transmitted through many

This work was submitted on Oct 25, 2024. This work was supported by a grant from Axis Bank Center for Mathematics and Computing and a startup grant from SERB-DST (SRG/2022/000163).

P. Dewan is with the Center for Condensed Matter Theory, Department of Physics, Indian Institute of Science, Bengaluru, Karnataka, India, PIN 560012. (e-mail: phanindrad@iisc.ac.in).

S. Sarkar is with the Center for Condensed Matter Theory, Department of Physics, Indian Institute of Science, Bengaluru, Karnataka, India, PIN 560012. (e-mail: sumantra@iisc.ac.in).

intermediate steps, where molecules are often transmitted diffusively [38]. Conversely, all long-distance communication in eukaryotes is carried by molecular motors. A well-known example is the transmission of signals through axon [36, 39].

In this paper, we explore the role of active, nonequilibrium transport in MC channels in two manifestations and investigate their consequences in the context of 1D channels. Specifically, we have considered channels where active transport happens (a) through static molecular relays and (b) through a mixture of active and passive particles. Physically, case (a) investigates the variation of MI with the strength of *extrinsic* nonequilibrium drive, and case (b) investigates the same for *intrinsic* drives. These scenarios have been motivated by experimental observations and prior theoretical works. Studies have shown that information transmission in cells might be improved by having relays, in which a molecule can trigger the release of the same type of molecule [35, 40]. Relay signaling motifs in neutrophils can lead to diffusive information waves [35]. In fact, MC through active transport can be a way of using aspects of communication theory to understand biological signaling networks [41].

II. METHODS

A. Model

We consider a simple one-dimensional (1D) model of molecular communication, where a diffusible molecule stochastically moves from a transmitter to a receiver through a 1D channel. The model and its consequences have been described earlier in ref. [34]. Here we summarize the main results for the sake of completeness. In this model (Fig. 1), transport happens on a 1D lattice, where molecules jump towards the receiver (to the right) with rate k_R and towards the transmitter (to the left) with rate k_L . For the sake of simplicity, it is assumed that once transmitted, the transmitter cannot reabsorb the molecules, and, once detected, the molecules cannot be emitted back to the lattice by the receiver. These two criteria are accommodated through reflecting boundary conditions at $x = 0$ and absorbing boundary conditions at $x = L$, respectively. The molecules are featureless particles that interact via excluded volume interaction. Hence, only one molecule can occupy a lattice point at a time.

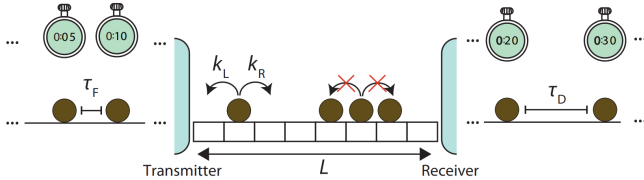


Fig. 1. Schematic diagram of the model. [34]

Molecules are emitted or fired from the transmitter at different times, and the intervals between firing times of two consecutive molecules are the firing time intervals and are defined as $\tau_F = t_F^{i+1} - t_F^i$. The time interval between two consecutive detection events at the receiver is the detection time interval and is defined as $\tau_D = t_D^{j+1} - t_D^j$. t_F^i is the

firing time of i^{th} firing event and t_D^j is the detection time of the j^{th} detection event.

We assume that the information is stored in the time interval between firing events, τ_F , which is a realistic assumption in many biological systems. For example, it is possible to estimate the concentration of molecules by counting how often ligands bind to a receptor. Each binding event may trigger downstream signaling, which will be analogous to a firing event in our model [42]. The detection time interval, τ_D , is the information received after traveling through the molecular communication channel. Because of the stochastic transport of the information carrier molecules, τ_D will be statistically different from τ_F . Following the industry-standard [43], we estimate the efficacy of information transmission by computing the mutual information between τ_F and τ_D , defined as [44, 45]:

$$I(\tau_F, \tau_D) = \sum_{\tau_F} \sum_{\tau_D} P(\tau_F; \tau_D) \ln \frac{P(\tau_F; \tau_D)}{P(\tau_F)P(\tau_D)} \quad (1)$$

$$= \sum_{\tau_F} \sum_{\tau_D} P(\tau_F) P(\tau_D | \tau_F) \ln \frac{P(\tau_D | \tau_F)}{P(\tau_D)} \quad (2)$$

where $P(\tau_F)$ is the firing time distribution, $P(\tau_D)$ is the detection time distribution, and $P(\tau_F; \tau_D)$ is the joint distribution of firing time interval and detection time interval. To compare our results across various firing time distributions, we normalized the mutual information by its maximum value, $H(\tau_F)$:

$$I = \frac{I(\tau_F; \tau_D)}{H(\tau_F)} \quad (3)$$

where $H(\tau_F)$ is the Shannon entropy of the firing time distribution, defined as

$$H(\tau_F) = - \sum_{\tau_F} P(\tau_F) \ln P(\tau_F) \quad (4)$$

We have carried out stochastic simulations for the 1D model and stored the firing time interval and detection time interval data. In general, the estimation of MI from samples of two random variables is not an easy problem. However, using methods in [45], we can obtain the MI between τ_F and τ_D [34]. It is important to note that below a certain threshold for the MI values, of the order of 10^{-3} to 10^{-4} , MI calculated using this method [45] does not give a good estimation. Also, the minimum sample size for firing and detection time intervals was kept at 10000, keeping in mind that current algorithms to calculate MI are strongly sample-size-dependent [34, 45].

B. Information transmission in bare channels

In [34], we studied the variation of I with the different parameters of the model. The most striking observation was that the variation of I depended only on a dimensionless parameter, called the Peclet number $Pe = vL/D$, where $v = a(k_R - k_L)$ is the drift velocity and $D = a^2(k_R + k_L)/2$ is

the diffusion coefficient of the molecules. Specifically, $I(Pe)$ showed three clear regimes:

$$I(Pe) = \begin{cases} Pe^0 & Pe < Pe_0 = \frac{2v\tau_F}{L} \\ Pe^{-4} & Pe_0 \leq Pe < 1 \\ Pe^{-1} & Pe \geq 1 \end{cases} \quad (5)$$

At $Pe = 1$, molecular transport transitions from a diffusion-dominated regime to an advection-dominated regime. Hence, the concurrent transition in $I(Pe)$ at $Pe = 1$ indicates its strong dependence on the transport processes that drive the molecular communication channel. Hence, in this paper, our main goal is to explore information transmission through two modes of molecular transport processes: relays, and active transport.

C. Relays

In our model, *relays*, as inspired by biological systems [35, 40], are special points on the one-dimensional lattice which can alter the hopping rates of the molecules shown in Fig. 3a. Once a molecule hops to a relay, say at site i , then it is always pushed to the next lattice point, $i + 1$, towards the receiver, as long as the next lattice point is empty.

D. Active Particles

In a second model, we include mixtures of *active* and *passive* particles, which are defined below. Active particles consume chemical energy and convert it to mechanical motion, which endows them with directional motility [37]. Molecular motors, such as myosin and kinesin, are examples of self-propelled particles. We model an active particle with totally asymmetric hopping rates, which are $k_L = 0$ and $k_R = 1$ in this paper. In contrast, passive particles, such as diffusing molecules, have symmetric hopping rates ($k_L = k_R = 1$) and undergo an unbiased 1D random walk. We vary the fraction of active particles, f_a , in the mixture and study its impact on the information transmission.

Kymographs: In order to visualize the stochastic trajectories of particles on the lattice, we will show kymographs of the particles, which is a visual representation of each individual particle's position along the x-axis, and time along the y-axis. The path a particle traces out on the lattice is then plotted in this $x - t$ plane. Kymographs also give an intuitive picture of the crowding in the channel.

Cluster size: Passive particles bounded by active particles can form clusters due to the totally asymmetric movement of the latter, which impact their transport and the transport of the associated information. Hence, it is necessary to identify the cluster and their sizes, which is a relatively easy task for 1D channels. There, such clusters will essentially be a configuration of the form $APPPP...PA$, with A denoting an active particle and P denoting a passive particle. The detection time interval, τ_D , between two successive particles in a cluster is equal to 1, even though their τ_F is usually different from 1. The size of a cluster in our model is then the length of the string of 1's in the detection time interval data. We have measured the unconditional cluster size distribution for

different active fractions and also the distribution conditioned on $\tau_F \neq 1$. The difference between these distributions are insignificant. Hence, we have shown the unconditional cluster size distribution in this paper.

III. RESULTS

A. Channels with one relay obey data processing inequality

To establish our model, we first describe the variation of mutual information in the presence of just one relay. In this setup, we can characterize the information channel through three different MI for three different transport processes. We denote the MI between the transmitter and the relay as I_1 , between the relay and the receiver as I_2 , and between the transmitter and receiver as I_3 . Because the transport of the molecules is memoryless in the channel, the three processes above form a Markov chain (see Fig. 2a). For a Markov chain $X \rightarrow Y \rightarrow Z$, the *data processing inequality* holds, which states that: $I(X; Y) \geq I(X; Z)$ [44]. Here, $I(X; Y)$ is the mutual information between the random variables X and Y , and $I(X; Z)$ is the mutual information between X and Z . As shown in Fig. 2b, I_1 is always greater than I_3 for all system sizes explored in our 1D model, which is a direct demonstration of the data processing inequality in our model. Hence, we can assume that the model is consistent with existing models of information transmission.

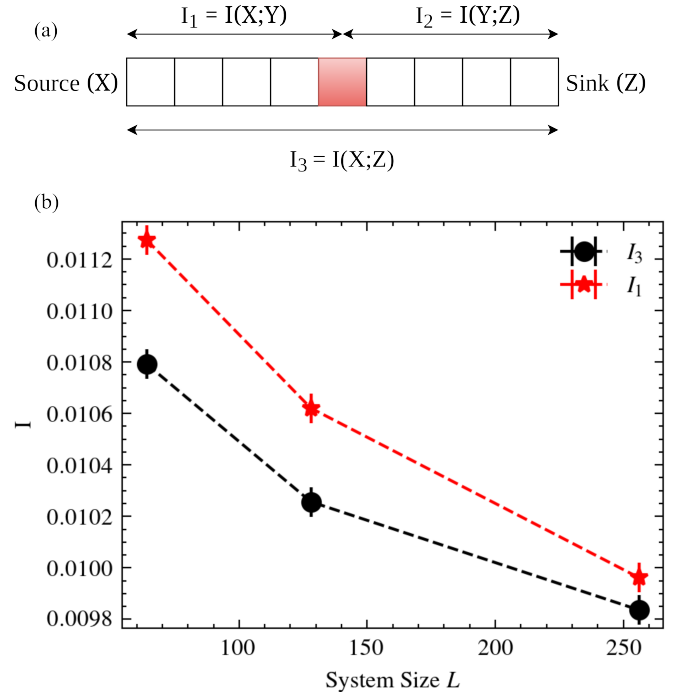


Fig. 2. (a) Schematic of the one relay lattice. The red site is the relay. (b) I_1 and I_3 vs. system size for channels with *one* relay. The relay is kept at the midpoint of the 1D channel.

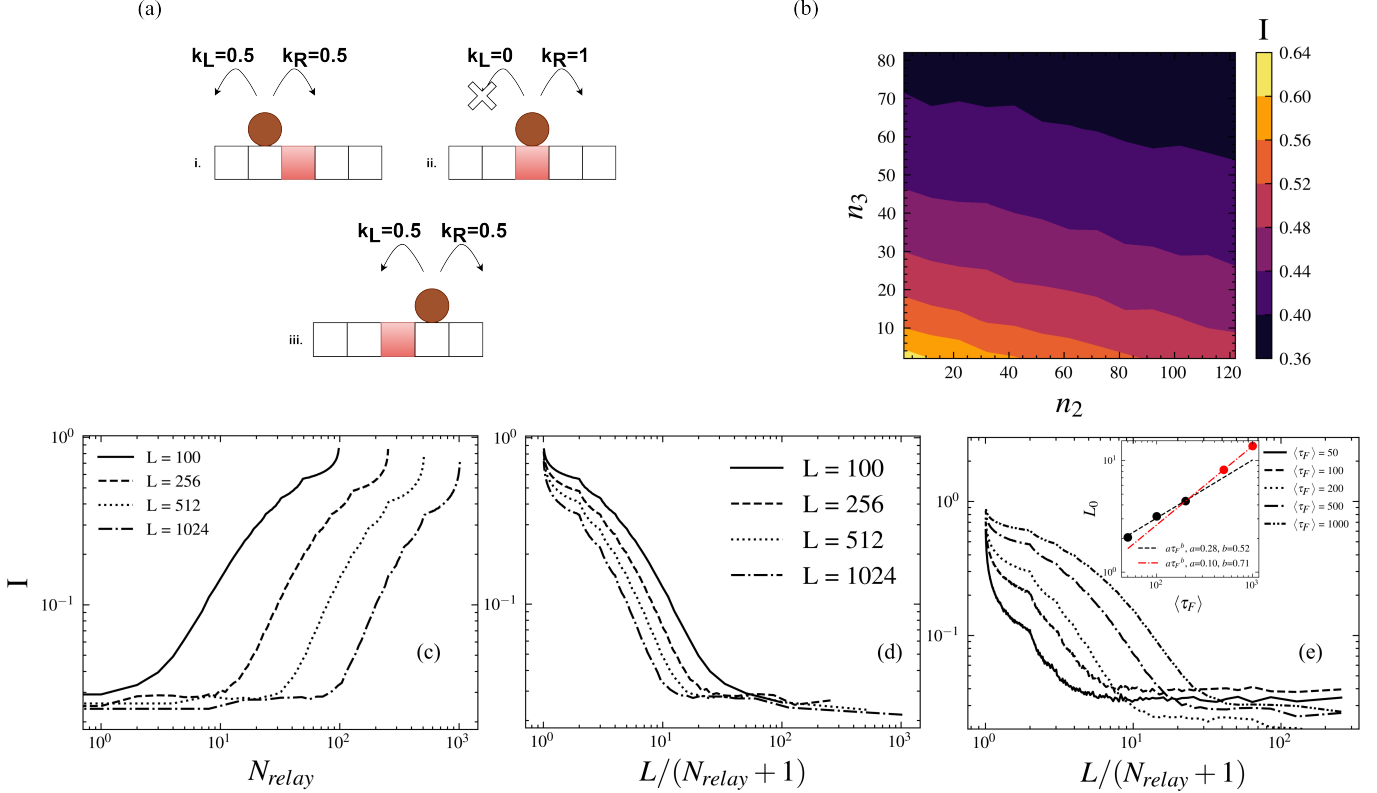


Fig. 3. (a) Schematic diagram of relays. The site coloured red is the relay site. (i) A molecule (labeled in brown) approaches the relay site. Its left and right hopping rates are equal, in this case: $k_L = 0.5$, $k_R = 0.5$. (ii) The molecule reaches the relay site, and its hopping rates change to $k_L = 0$ and $k_R = 1$. (iii) The molecule is pushed by the relay into the next site, where its hopping rates change back to $k_L = 0.5$ and $k_R = 0.5$. (b) A contour plot showing the variation of I , the MI between transmitter-receiver, with n_2 and n_3 , where n_2 is the number of DCs of length 2 and n_3 is the number of DCs of length 3 in the channel. (c) Variation of MI between source-sink with inter-relay distance for different lengths of the 1D lattice. (d) Variation of MI between source-sink with number of relays for different lengths of the 1D lattice. (e) Variation of MI between source-sink with inter-relay distance for different $\langle \tau_F \rangle$, with $L = 256$. Inset shows variation of threshold length L_0 with $\langle \tau_F \rangle$. Here, L_0 is the threshold inter-relay distance $L/(N_{relay} + 1)$ at which I falls below 0.1 in (d).

B. Channels with many relays are nontrivial information transporters

It may be possible to achieve better transmission quality by introducing multiple relays. For example, wireless repeaters can reduce black spots in a wifi network. Also, it has been observed that relay motifs in neutrophils help spread information through diffusive waves [35]. These observations led us to explore the dependence of MI on the number of relays, N_{relay} , in the channel. This dependence is nontrivial. In the absence of any relays, the channel is purely diffusive and has low efficacy, characterized by a system-size (L) dependent MI value. As the number of relays increases, MI does not increase until an L -dependent threshold number of relays, above which it increases non-linearly through repeated exponential rise up to the maximum value of 1 (Fig. 3c).

Upon closer inspection, we found that the exponential jumps happen when the inter-relay distance is not an integer. For example, if we plot the MI as a function of inter-relay distance ($L/(N_{relay} + 1)$), it becomes clear that the end-points of the exponential variations are characterized by integer inter-relay distance, which implies that the distance between all consecutive relays are equal. When the distance is not an integer, then there are spatial variations in the channel length.

In both cases, the total loss of information is a nonlinear aggregate of the loss in individual DCs present between two consecutive relays. Information loss in a DC of length l goes as l^{-4} above a threshold length and as l^0 below this threshold, $L_0 = \sqrt{2D\langle \tau_F \rangle}$ [34].

To understand whether L_0 is also the threshold for the nonlinear increase of MI, we computed its variation with inter-relay distance for various values of $\langle \tau_F \rangle$ shown in Fig. 3e. Indeed, the threshold inter-relay distance increases as $\langle \tau_F \rangle^{1/2}$ for small values of τ_F , but shows steeper increase at higher values of $\langle \tau_F \rangle$ (Fig. 3e inset). This observation suggests that L_0 does govern the threshold inter-relay distance, albeit for a limited range of $\langle \tau_F \rangle$ values. Beyond this insight, unfortunately, we could not find any simple relation between the number of DCs and the information loss. Generalizing the data processing inequality to the multi-relay scenario provided a weak upper bound on the information loss in the entire channel, which was practically unusable. Therefore, we sought to understand the cases where the length of individual DCs was small.

C. Information loss in small diffusive channels follows a stretched exponential law

DCs of varying lengths are the building blocks of the lattice channel with relays. When the inter-relay distance is an integer, the channels are of equal length. For example, when the inter-relay distance changes from 1 to 2, the number of DCs of length 2, say n_2 , increases from 0 to 64 for a lattice of length 128. Thus, the decrease in MI as inter-relay distance increases is equivalent to the decrease in MI due to an increase in the number of DCs of length 2, n_2 . Simulation results with channels made of single-length DCs (of lengths 2, 3, 5, and 10) suggested that the MI between the transmitter and receiver made up of DCs of length l is given by a stretched exponential function [Fig. 4]:

$$I(n_l) = e^{-\left(\frac{n_l}{\alpha}\right)^\mu} \quad (6)$$

where,

n_l = number of diffusive channels of length l

μ = stretching exponent

$$\alpha = (\ln(1/I(1)))^{-\frac{1}{\mu}}$$

l	μ	α
2	0.291	353.264
3	0.273	66.585
5	0.261	8.459
10	0.251	0.564

TABLE I

μ AND α FOR DIFFERENT DIFFUSIVE CHANNEL BLOCK LENGTHS, l .

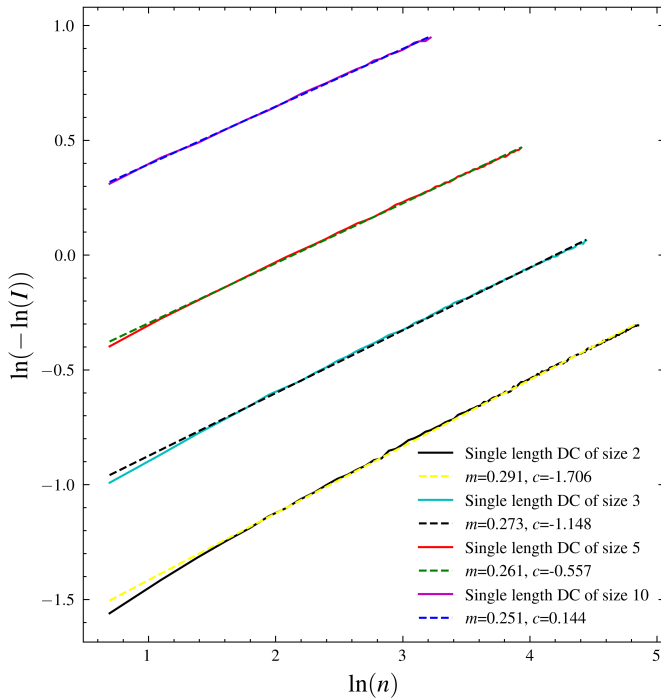


Fig. 4. Plot of $\ln(-\ln I)$ vs. $\ln n$, which shows that channels made of single-length DCs of lengths 2, 3, 5, 10 all follow the stretched exponential function given in Eq. 6. A straight line is fitted to the simulation data, with the slope, m and intercept c given in the legend.

D. Differential dependence on block length in mixed relay channels

The dependence of MI for DCs of a fixed length with no relays was shown before [34], but to understand the dependence of MI on N_{relay} , we need to understand the dependence of MI for lattice channels with DCs of different lengths, interspersed with relays. This seems to be a difficult task as it is not clear what the functional dependence of MI will be on n_l , where n_l is the number of DCs of length l . To gain insight, we performed simulations by varying n_2 and n_3 in mixed channels of length $L = 2n_2 + 3n_3$. As shown in Figure 3f, the dependence of MI on n_3 is much stronger than on n_2 ; roughly, 10 size-3 (total length 30) channels reduce the information by the same amount as 40 size-2 channels (total length 80). This is physically understandable as DCs of length 3 are more likely to decorrelate the molecular transport than DCs of length 2.

E. Increasing active fraction leads to nonlinear increase in MI

MI increases non-linearly with active fraction, f_a , in a manner (Fig. 5a) not unlike the relay channels (Fig. 3c). However, unlike the relay channels, neither the threshold active fraction ($f_a \approx 0.1$) nor the general trend depends on the total channel length. The origin of the threshold MI value, which is around 2×10^{-3} is unclear. Because the algorithm to compute MI has a resolution of $\sim 10^{-3}$ [45], the threshold can arise due to the inability of the algorithm to resolve MI variation below this limit. In contrast, the variation of MI above this threshold is well-defined and follows a power law: $MI \sim f_a^3$ (Fig. 5a).

$$I(f_a) = \begin{cases} f_a^0 & f_a \leq 0.1 \\ f_a^3 & f_a > 0.1 \end{cases} \quad (7)$$

Power law variation implies the presence of a strong correlation in the underlying phenomena. In MC channels, the transport of the molecules determines the variation in MI. Therefore, we suspected that the molecules were moving from the transmitter to the receiver through a collective transport process. Inspection of the joint distribution of τ_F and τ_D strengthened this hypothesis (Fig. 5b). We found that for $f_a = 0$, the distribution showed no correlation between the variables, and for $f_a = 1$, τ_D was proportional to τ_F . However, for the threshold value, $f_a = 0.1$, for a wide range of τ_F values the distribution of τ_D was centered at $\tau_D = 1$. This observation implied that even though the molecules were fired randomly, they reached the detector one after the other, i.e., in a collective fashion. Indeed, a measurement of the cluster size distribution revealed the presence of large clusters (cluster size of $\sim 20 - 50$) at small nonzero values of f_a , whereas the average cluster size was approximately 1 or 2 for $f_a = 0$ or 1 (Fig. 5c). We found visual support of this observation from the kymographs of the particles, which showed strong clustering for $f_a = 0.1$, but no clustering for $f_a = 0$ or 1 (Fig. 5d).

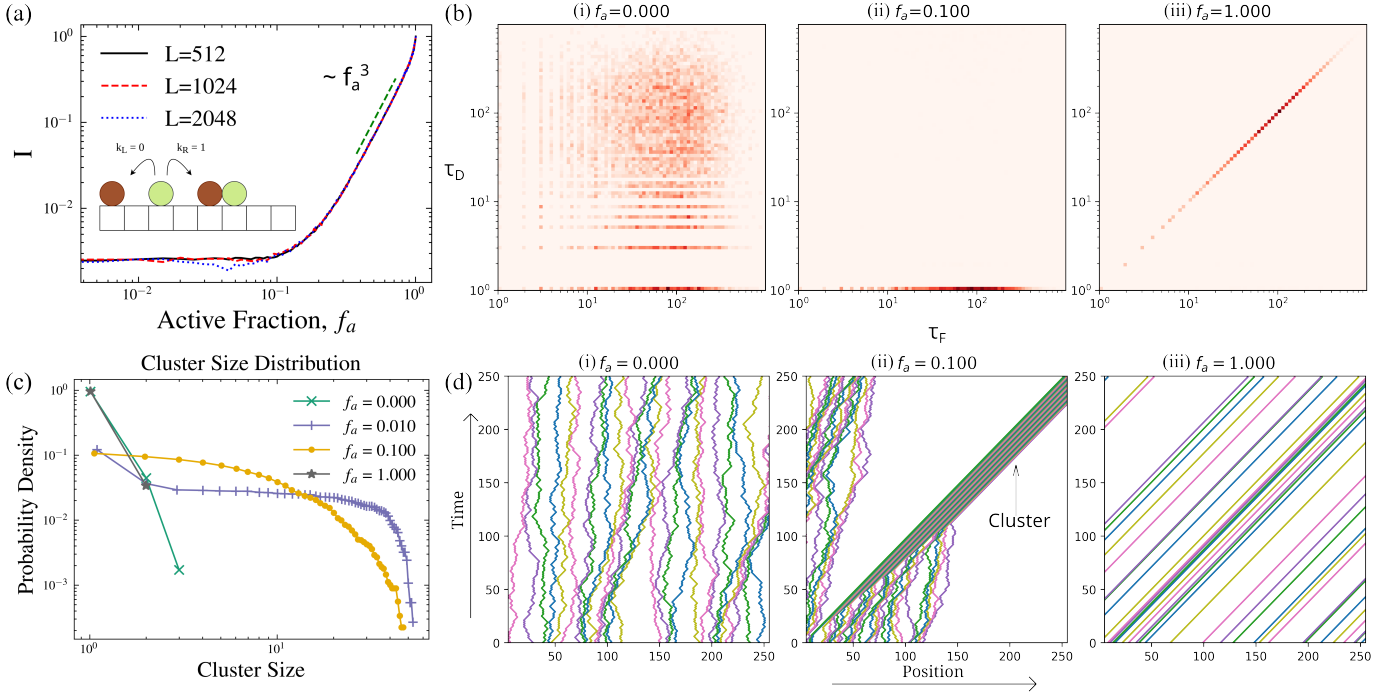


Fig. 5. (a) MI vs. active fraction for channels of different lengths, with $k_R = 1$ for active particles. The best fit shows that above an active fraction, $MI \sim f_a^3$. The inset shows a schematic showing active particles labeled green, with passive particles labeled brown. (b) The joint probability distribution function, $P(\tau_F, \tau_D)$ for different active fractions, f_a . (i) $f_a = 0$, (ii) $f_a = 0.1$, (iii) $f_a = 1$. (c) Cluster size distribution for different active fractions f_a . (d) Kymographs from stochastic simulations. Kymographs show molecular trajectories for different active fractions, (i) $f_a = 0$, (ii) $f_a = 0.1$, and (iii) $f_a = 1$, all for $L = 256$.

IV. CONCLUSION

In this paper, we have investigated how the active transport of information molecules affects molecular communication in a simple 1D model of molecular communication, proposed in [34]. In this model, we assumed that the information is encoded in the time interval between two consecutive detection events at the receiver, τ_D , which were transmitted from the transmitter with some known time interval distribution, τ_F . We measured the efficacy of the molecular communication channel through the mutual information, $I(\tau_F; \tau_D)$, between τ_F and τ_D in two models of active transport.

Our main conclusion is that the crowding of the molecules in the channel is the key driver of the efficacy. Only in the limit of rare firing events ($\tau_F \gg 1$) the active or passive nature of the communication channel becomes important. A striking example of this observation is shown in Fig. 5, which shows the transition of the joint probability distribution with the fraction of active particles, f_a . At $f_a \approx 0.1$, $I(\tau_F; \tau_D)$ starts to increase rapidly. The joint probability distribution at the transition point shows that $\tau_D = 1$ for almost all values of τ_F . Such extreme distribution arises because of the effect of crowding and the resultant collective transport. At this f_a , the configurations are such that the channel gets crowded rapidly, and the particles can only move forward because of their excluded volume interactions. This interaction results in a single file movement where particles reach the receiver immediately after one another.

The effect of crowding is also important for the relays, where crowding, predominantly present at low values of

$\langle \tau_F \rangle$, reduces the mutual information (Fig. 3e). This result is counterintuitive but can be explained through the following reasoning. Intuitively, in DCs, we expect the crowding to reduce the noise due to diffusive movements. However, the presence of relays and the crowding together completely suppress the diffusive movement. Naively, we expect this effect to increase the MI. However, strong crowding and the relays can make $P(\tau_D)$ a narrowly peaked distribution, which is quite different from the exponential $P(\tau_F)$. Hence, MI can be reduced due to the effect of crowding. It seems that the relays and the active particles have opposing reactions to the crowding of molecules, in addition to their inherent differences in the nature of the nonequilibrium drive. It will be interesting to investigate the combined effects of these special cases. However, that is a formidable task and is beyond the scope of the current manuscript.

In conclusion, we sought to investigate the differential effects of active and passive transport in various conditions and found that crowding is the main driver of the efficacy of information transmission. Therefore, to design better molecular communication channels, we should understand the effects of crowding. Crowding is a challenging problem to tackle analytically, as it introduces memory effects. However, in some circumstances, crowding and its effects can be analyzed through analytical techniques [46]. Applying these results in the context of molecular communication will be useful and potentially important.

REFERENCES

- [1] N. Farsad, H. B. Yilmaz, A. Eckford, C.-B. Chae, and W. Guo, "A comprehensive survey of recent advancements in molecular communication," *IEEE Communications Surveys & Tutorials*, vol. 18, no. 3, pp. 1887–1919, 2016.
- [2] N. Farsad, W. Guo, and A. W. Eckford, "Tabletop molecular communication: Text messages through chemical signals," *PLoS one*, vol. 8, no. 12, p. e82935, 2013.
- [3] M. Gregori and I. F. Akyildiz, "A new nanonetwork architecture using flagellated bacteria and catalytic nanomotors," *IEEE Journal on selected areas in communications*, vol. 28, no. 4, pp. 612–619, 2010.
- [4] L. C. Cobo and I. F. Akyildiz, "Bacteria-based communication in nanonetworks," *Nano Communication Networks*, vol. 1, no. 4, pp. 244–256, 2010.
- [5] S. Hiyama, R. Gojo, T. Shima, S. Takeuchi, and K. Sutoh, "Biomolecular-motor-based nano-or microscale particle translocations on dna microarrays," *Nano Letters*, vol. 9, no. 6, pp. 2407–2413, 2009.
- [6] S. Hiyama, Y. Moritani, R. Gojo, S. Takeuchi, and K. Sutoh, "Biomolecular-motor-based autonomous delivery of lipid vesicles as nano-or microscale reactors on a chip," *Lab on a Chip*, vol. 10, no. 20, pp. 2741–2748, 2010.
- [7] S. Hiyama and Y. Moritani, "Molecular communication: Harnessing biochemical materials to engineer biomimetic communication systems," *Nano Communication Networks*, vol. 1, no. 1, pp. 20–30, Mar. 2010. [Online]. Available: <http://www.sciencedirect.com/science/article/pii/S1878778910000074>
- [8] A. Enomoto, M. J. Moore, T. Suda, and K. Oiwa, "Design of self-organizing microtubule networks for molecular communication," *Nano Communication Networks*, vol. 2, no. 1, pp. 16–24, 2011.
- [9] T. Nitta, A. Tanahashi, M. Hirano, and H. Hess, "Simulating molecular shuttle movements: Towards computer-aided design of nanoscale transport systems," *Lab on a Chip*, vol. 6, no. 7, pp. 881–885, 2006.
- [10] T. Nitta, A. Tanahashi, and M. Hirano, "In silico design and testing of guiding tracks for molecular shuttles powered by kinesin motors," *Lab on a Chip*, vol. 10, no. 11, pp. 1447–1453, 2010.
- [11] K. E. Byun, K. Heo, S. Shim, H. J. Choi, and S. Hong, "Functionalization of silicon nanowires with actomyosin motor protein for bioinspired nanomechanical applications," *Small*, vol. 5, no. 23, pp. 2659–2664, 2009.
- [12] J. Ikuta, N. K. Kamisetty, H. Shintaku, H. Kotera, T. Kon, and R. Yokokawa, "Tug-of-war of microtubule filaments at the boundary of a kinesin-and dynein-patterned surface," *Scientific reports*, vol. 4, no. 1, p. 5281, 2014.
- [13] D. Steuerwald, S. M. Früh, R. Griss, R. D. Lovchik, and V. Vogel, "Nanoshuttles propelled by motor proteins sequentially assemble molecular cargo in a microfluidic device," *Lab on a Chip*, vol. 14, no. 19, pp. 3729–3738, 2014.
- [14] M. J. Moore, T. Suda, and K. Oiwa, "Molecular communication: Modeling noise effects on information rate," *IEEE transactions on nanobioscience*, vol. 8, no. 2, pp. 169–180, 2009.
- [15] N. Farsad, A. W. Eckford, S. Hiyama, and Y. Moritani, "A simple mathematical model for information rate of active transport molecular communication," in *2011 IEEE conference on computer communications workshops (INFOCOM WKSHPs)*. IEEE, 2011, pp. 473–478.
- [16] N. Farsad, A. W. Eckford, and S. Hiyama, "A mathematical channel optimization formula for active transport molecular communication," in *2012 IEEE International Conference on Communications (ICC)*. IEEE, 2012, pp. 6137–6141.
- [17] —, "A markov chain channel model for active transport molecular communication," *IEEE Transactions on Signal Processing*, vol. 62, no. 9, pp. 2424–2436, 2014.
- [18] J. Selimkhanov, B. Taylor, J. Yao, A. Pilko, J. Albeck, A. Hoffmann, L. Tsimring, and R. Wollman, "Accurate information transmission through dynamic biochemical signaling networks," *Science*, vol. 346, no. 6215, pp. 1370–1373, Dec. 2014, publisher: American Association for the Advancement of Science Section: Report. [Online]. Available: <https://science.sciencemag.org/content/346/6215/1370>
- [19] —, "Accurate Information Transmission Through Dynamic Biochemical Signaling Networks," *Science*, vol. 346, no. 6215, pp. 1370–1373, Dec. 2014. [Online]. Available: <https://www.ncbi.nlm.nih.gov/pmc/articles/PMC4813785/>
- [20] G. Aminian, H. Arjmandi, A. Gohari, M. Nasiri-Kenari, and U. Mitra, "Capacity of Diffusion-Based Molecular Communication Networks Over LTI-Poisson Channels," *IEEE Transactions on Molecular, Biological and Multi-Scale Communications*, vol. 1, no. 2, pp. 188–201, Jun. 2015, conference Name: IEEE Transactions on Molecular, Biological and Multi-Scale Communications.
- [21] M. Pierobon and I. F. Akyildiz, "Capacity of a Diffusion-Based Molecular Communication System With Channel Memory and Molecular Noise," *IEEE Trans. Inform. Theory*, vol. 59, no. 2, pp. 942–954, Feb. 2013. [Online]. Available: <http://ieeexplore.ieee.org/document/6305481/>
- [22] D. Arifler, "Capacity analysis of a diffusion-based short-range molecular nano-communication channel," *Computer Networks*, vol. 55, no. 6, pp. 1426–1434, Apr. 2011. [Online]. Available: <http://www.sciencedirect.com/science/article/pii/S1389128610003919>
- [23] N. Hao, B. A. Budnik, J. Gunawardena, and E. K. O'Shea, "Tunable signal processing through modular control of transcription factor translocation," *Science*, vol. 339, no. 6118, pp. 460–464, Jan. 2013.
- [24] A. Hoffmann, A. Levchenko, M. L. Scott, and D. Baltimore, "The IkkappaB-NF-kappaB signaling module: temporal control and selective gene activation," *Science*, vol. 298, no. 5596, pp. 1241–1245, Nov. 2002.
- [25] S. D. M. Santos, P. J. Verveer, and P. I. H. Bastiaens, "Growth factor-induced MAPK network topology shapes Erk response determining PC-12 cell fate," *Nat. Cell Biol.*, vol. 9, no. 3, pp. 324–330, Mar. 2007.
- [26] J. E. Purvis and G. Lahav, "Encoding and decoding

- cellular information through signaling dynamics,” *Cell*, vol. 152, no. 5, pp. 945–956, Feb. 2013.
- [27] W. H. de Ronde, F. Tostevin, and P. R. ten Wolde, “Effect of feedback on the fidelity of information transmission of time-varying signals,” *Phys Rev E Stat Nonlin Soft Matter Phys*, vol. 82, no. 3 Pt 1, p. 031914, Sep. 2010.
- [28] F. Tostevin and P. R. ten Wolde, “Mutual information between input and output trajectories of biochemical networks,” *Phys. Rev. Lett.*, vol. 102, no. 21, p. 218101, May 2009.
- [29] P. B. Dieterle, J. Min, D. Irimia, and A. Amir, “Dynamics of diffusive cell signaling relays,” *bioRxiv*, p. 2019.12.27.887273, Dec. 2019, publisher: Cold Spring Harbor Laboratory Section: New Results. [Online]. Available: <https://www.biorxiv.org/content/10.1101/2019.12.27.887273v1>
- [30] R. Cheong, A. Rhee, C. J. Wang, I. Nemenman, and A. Levchenko, “Information transduction capacity of noisy biochemical signaling networks,” *Science*, vol. 334, no. 6054, pp. 354–358, Oct. 2011.
- [31] G. Tkačik and W. Bialek, “Information Processing in Living Systems,” *Annual Review of Condensed Matter Physics*, vol. 7, no. 1, pp. 89–117, 2016, _eprint: <https://doi.org/10.1146/annurev-conmatphys-031214-014803>. [Online]. Available: <https://doi.org/10.1146/annurev-conmatphys-031214-014803>
- [32] P. Dieterle, J. Min, D. Irimia, and A. Amir, “Dynamics of diffusive cell signaling relays,” *bioRxiv*, 2019.
- [33] S. Kadloor, R. S. Adve, and A. W. Eckford, “Molecular communication using brownian motion with drift,” *IEEE Transactions on NanoBioscience*, vol. 11, no. 2, pp. 89–99, 2012.
- [34] S. Sarkar, M. Z. Ali, and S. Choubey, “Efficacy of information transmission in cellular communication,” *Physical Review Research*, vol. 5, no. 1, p. 013092, 2023.
- [35] P. B. Dieterle, J. Min, D. Irimia, and A. Amir, “Dynamics of diffusive cell signaling relays,” *Elife*, vol. 9, p. e61771, 2020.
- [36] R. Phillips, J. Kondev, J. Theriot, and H. Garcia, *Physical biology of the cell*. Garland Science, 2012.
- [37] S. Ramaswamy, “The mechanics and statistics of active matter,” *Annu. Rev. Condens. Matter Phys.*, vol. 1, no. 1, pp. 323–345, 2010.
- [38] W. Lim, B. Mayer, and T. Pawson, *Cell signaling*. Taylor & Francis, 2014.
- [39] R. Milo, P. Jorgensen, U. Moran, G. Weber, and M. Springer, “Bionumbers—the database of key numbers in molecular and cell biology,” *Nucleic acids research*, vol. 38, no. suppl_1, pp. D750–D753, 2010.
- [40] J. Strickland, D. Pan, C. Godfrey, J. S. Kim, A. Hopke, M. Degrange, B. Villavicencio, M. K. Mansour, C. S. Zerbe, D. Irimia *et al.*, “Self-extinguishing relay waves enable homeostatic control of human neutrophil swarming,” *bioRxiv*, 2023.
- [41] T. Nakano, “Molecular communication: A 10 year retrospective,” *IEEE Transactions on Molecular, Biological and Multi-Scale Communications*, vol. 3, no. 2, pp. 71–78, 2017.
- [42] P. Mehta and D. J. Schwab, “Energetic costs of cellular computation,” *Proceedings of the National Academy of Sciences*, vol. 109, no. 44, pp. 17978–17982, 2012.
- [43] G. Tkačik and W. Bialek, “Information processing in living systems,” *Annual Review of Condensed Matter Physics*, vol. 7, pp. 89–117, 2016.
- [44] T. M. Cover, *Elements of information theory*. John Wiley & Sons, 1999.
- [45] C. M. Holmes and I. Nemenman, “Estimation of mutual information for real-valued data with error bars and controlled bias,” *Physical Review E*, vol. 100, no. 2, p. 022404, 2019.
- [46] K. Mallick, “The exclusion process: A paradigm for non-equilibrium behaviour,” *Physica A: Statistical Mechanics and its Applications*, vol. 418, pp. 17–48, 2015.